Effect of Bimodal Molecular Weight Distribution on the Polymer Brush

N. Dan*,† and M. Tirrell

Department of Chemical Engineering and Material Science, University of Minnesota, Minneapolis, Minnesota 55455

Received May 12, 1993; Revised Manuscript Received August 16, 1993®

ABSTRACT: A numerical self-consistent-field model is used to calculate the equilibrium properties of an end-grafted polymer "brush" with a bimodal molecular weight distribution immersed in a good solvent. We find that the longer chains stretch significantly more than the shorter chains in the region near the interface, irrespective of the molecular weight difference or composition. As a result, vertical segregation between the segments of the shorter and longer chains occurs. In systems where the difference in molecular weight between the two chains is small, the longer chain ends are localized at the brush edge. Segment density profiles of two symmetrical brushes compressed together show that stratification persists under compression. The effect of finite molecular weight on the bimodal brush structure is similar to that in monodisperse systems. However, there is also an unpredicted, strong dependency of various aspects of chain configuration on the molecular weight ratio and composition of the bimodal brush.

Introduction

Polymer brushes are composed of chains that are attached, or grafted, by one end to an impenetrable, usually noninteracting interface. In systems where the grafting is dense, i.e., the distance between graft points is small compared to the polymer chain dimensions, strong overlap among neighboring chains is enforced. Consequently, the chains deform and stretch in the direction perpendicular to the interface forming a "brushlike" structure.[1-4] Applicability to colloidal stabilization, surface modifiers, adhesives, and polymeric amphiphiles has led to extensive study of these systems.[1,2]

Enhanced performance of polymeric brushes requires fine control of brush parameters. Most applications involve either direct interactions (for example, in adhesion) or response to flow (such as in colloid stabilization). Both interactions and hydrodynamic response are governed, to a large extent, by the properties of the outer brush edge.[5,6] Successful utilization of polymeric brushes necessitates, therefore, control of the outer brush structure.

Polydispersity, which is an important, and often unavoidable, feature of polymer systems, has been shown to affect the brush structure strongly.[7-11] An understanding of the relationship between the molecular weight distribution and the brush properties is thus essential. Moreover, an imposed molecular weight distribution may be thereby used to engineer the brush structure according to specific needs. A monodisperse brush has only two controllable parameters, namely, the chain molecular weight and the grafting density.[1-4] However, a controlled molecular weight distribution offers a larger number of variables. The polydisperse brush structure can thus be tailored to specifications.

Of special interest is possible localization of specific chain ends at the outer brush edge. In the monodisperse brush, most of the chain ends are buried in the brush interior, and there is no control over the small fraction of ends which does extend to the outer brush. On the other hand, in a polydisperse brush there may be a way of forcing certain chain ends (for example, the ends of the longest chains) to the outer surface.[8,9] By placing a particular functional group only on those protruding chain ends, the outer brush surface could be economically modified to perform desired functions (e.g., specific binding or adhesion). The brush affinity to other surfaces and response to flow can thereby be controlled without affecting the interior brush structure, thereby maintaining, for example, a robust steric barrier.

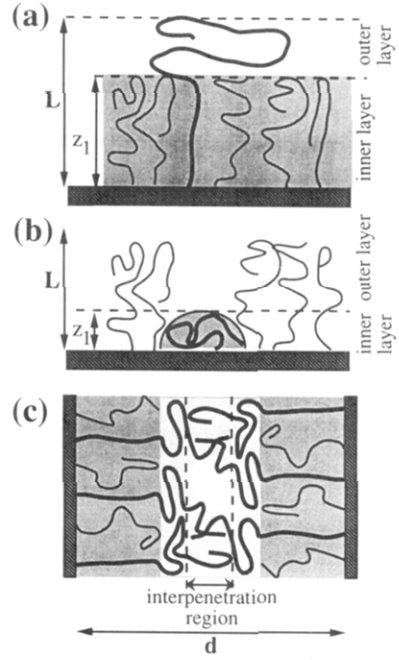

Figure 1. Biomodal brushes. (a) A longer test chain in a short-chain brush: The longer chain stretched through the inner region adjacent to the surface, thereby reducing the interaction energy. (b) A shorter test chain in a longer chain brush: The shorter chain is immersed in a nearly uniform environment, so that stretching would not reduce the interaction energy. Collapse, on the other hand, leads to a gain in entropy. (c) Interactions between compressed bimodal brushes. The interpenetration region is that where chain segments from both brushes overlap.

In this paper, we investigate a bimodal molecular weight distribution as a model system for polydispersity. A bimodal brush consists of a mixture of shorter and longer chains and can be crudely divided into two regions: the inner layer, which is adjacent to the surface and contains both short- and long-chain segments, and the outer layer, which contains only segments of the longer chains (Figure 1). In a good solvent, the configurations of densely tethered chains are determined by a balance between interaction energy and chain entropy, or elasticity.[3,4] The interaction energy increases with the local segment concentration,

† Present address: Department of Materials and Interfaces, Weizmann Institute, Rehovot 76100, Israel.

• Abstract published in *Advance ACS Abstracts,* October 15, 1993.

0024-9297/93/2226-6467$04.00/0

while entropy is inversely proportional to the degree of chain stretching. In a brush containing only a small fraction of longer chains (Figure 1a), the segment concentration in the outer brush is small. Strong stretching of the longer chains increases the number of segments in the dilute outer layer and, therefore, significantly reduces the interaction energy in the inner layer. The entropic loss due to additional long-chain stretching is, in this case, balanced by the gain in interaction energy. However, in a brush where a small fraction of the chains are shorter (Figure 1b), there is no significant concentration gradient between the inner and outer layers. The interaction energy of the shorter chain segments cannot be appreciably reduced by stretching, so that the short chains retain their random coil configuration.

The two main features of polydisperse brushes emerge from this qualitative discussion: vertical segregation between chains of different molecular weight, and the fact that coexisting shorter and longer chains may be distinguishable by their local degree of stretching.

The relationship between the molecular weight distribution and brush properties has been studied theoretically, using a self-consistent-field model (SCF)[8,9] for infinitely long chains. In SCF models, the configurations of the chains, and hence the monomer density distribution, are described as subject to a mean field, position-dependent chemical potential, arising self-consistently from the segment density profile.[12,13] The similarity between the dominant configuration of a strongly stretched chain and the trajectory of a classical particle can be employed to obtain an analytical segment density distribution function in this limit of high molecular weight. Brush properties, such as thickness and distribution of chain ends could then be calculated as a function of molecular weight distribution. The overall brush height was predicted to vary as[8,9,11]

$$L = \left(\frac{12v\sigma}{\pi^2}\right)^{1/3} N_1\{1 + \alpha\,(1-f)^{1/3}\} \qquad (1)$$

Here, σ is the dimensionless surface density, namely, the number of chains per unit area, and N_1 (N_2) is the molecular weight of the shorter (longer) chains. f is the fraction of shorter chains in the brush, and α is a measure of the molecular weight disparity, equal to $(N_2/N_1 - 1)$. The excluded volume parameter, v,[1,3,4] is unity in good solvents. It is important to note that, although in monodisperse brushes the thickness increases linearly with chain molecular weight, the bimodal brush thickness is not proportional to the average chain molecular weight, i.e., $fN_1 + (1-f)N_2$.

Vertical segregation between the short- and long-chain ends was predicted[8,9] to occur in the bimodal brush. The inner layer could thereby be defined as the region from which the longer chain ends were excluded, equal to[8,9,11]

$$z_1 = \left(\frac{12v\sigma}{\pi^2}\right)^{1/3} N_1\{1 - (1-f)^{2/3}\}^{1/2} \qquad (2)$$

The inner brush thickness is therefore expected to be independent of the molecular weight ratio, α. Similarly, the distribution of the shorter chain ends was also predicted to be independent of the longer chain molecular weight.[9,11] In the limit of low f, namely, a brush containing only a small fraction of shorter chains, the inner brush thickness goes to zero. The shorter chains are, therefore, expected to collapse completely in this limit.

These predictions have been tested, and to some degree confirmed, by Monte Carlo (MC) simulations.[10,11] However, the simulations were limited a narrow region of compositions ($0.25 < f < 0.75$) and to relatively low molecular weights, up to $N_2 = 60$. Investigation of the effect of finite molecular weight on the brush structure, which has been shown to be significant in monodisperse systems,[14,15] was thereby restricted. Especially important is the existence of a low-density "foot", which extends beyond the analytically predicted profile.[10,11,14,15] Although the size of the foot is negligible when compared to the brush height, foot composition and structure govern the outer brush properties and, hence, the hydrodynamic layer thickness and the interactions between surfaces.[5,6] Characterization of the brush foot region as a function of composition and molecular weight, which has not been done in the simulation studies,[10,11] is essential. Moreover, when two brushes come into contact, overlap occurs mainly in the foot region (see Figure 1c). In the analytical model, the lack of a foot region indicates that there will be no overlap between compressed brushes, and hence, the brush–brush interactions are strongly repulsive. However, in the finite molecular weight brush the compressed feet overlap to some extent, thereby softening the repulsive interactions and possibly producing important dynamic effects such as entanglement.[5] Understanding the behavior of compressed bimodal brushes is necessary if those are to be used as colloidal stabilizers or adhesives.

We examine in this work the effect of polydispersity and finite molecular weight on a grafted brush in a good solvent, using a bimodal molecular weight distribution as a model system. The Dolan–Edwards[12] self-consistent-field model of a grafted brush is modified to account for a molecular weight distribution and then solved numerically. This procedure enables investigation of high molecular weight, high surface density systems that cannot be explored by simulations, due to computing time limitations,[10,11] without assuming that the chains are of infinite molecular weight.[8,9] We calculate the properties of the bimodal brush as a function of the molecular weight of both chains and the brush composition, namely, the molar fraction of each chain. Also investigated is the effect of compression on the brush characteristics and the interactions between compressed brushes as manifested in the degree of interpenetration.

The Model

The configuration of a polymer segment in a system with excluded volume interactions is a function of the placement of all other segments in the system. In SCF models chain statistics are described as those of a random walk under an average potential field. The potential field, in turn, is a function of the segment distribution—hence, the self-consistency. In dilute and semidilute systems the potential is reasonably taken to be proportional to the local segment density (ϕ).[12,14,15]

We consider a bimodal polymer brush grafted at a (dimensionless) total density of σ chains per unit area. f is the fraction of shorter chains, so that the brush is composed of $(f\sigma)$ chains of N_1 and $(1-f)\sigma$ chains of N_2 molecular weight. The distribution function $Q(\mathbf{r},\mathbf{r}';n)$ denotes the statistical weight of a subchain starting at a spatial position $\mathbf{r}'$ and ending at position $\mathbf{r}$ in n steps, without crossing a confirning surface. Q satisfies the partial differential equation:

$$\frac{\partial Q}{\partial n} = \frac{a^2}{6}\nabla^2 Q - v\phi_{\mathrm{tot}}(\mathbf{r})\,Q(\mathbf{r},\mathbf{r}';n) \qquad (3)$$

The initial condition is given by $Q(\mathbf{r},\mathbf{r}';0) = \delta(\mathbf{r}-\mathbf{r}')$, and the boundary condition on the confining surface is $Q(\mathbf{r},\mathbf{r}';n) = 0$. The local monomer volume fraction, $\phi_{\mathrm{tot}}(\mathbf{r})$, consists

of contributions from both chains. At relatively high surface density, Q can be assumed to vary only with the direction perpendicular to the interface, depending on the segment number n and the height from the surface, z. v is taken in our calculation as 1, indicating a good solvent environment.

The average local segment density of each chain can be calculated by summing the probability of configurations passing through a spatial point:[12]

$$\phi_i(z) = \psi \frac{\int_0^{N_i} dn \int_0^{\infty} Q(0,z;n)\, Q(z,z';N_i-n)\, dz'}{\int_0^{\infty} Q(0,z';N_i)\, dz'} \quad (4)$$

where $i = 1$ or 2. The total segment density at height z, $\phi_{tot}(z)$, is equal to $\phi_1(z) + \phi_2(z)$. ψ is a normalization factor, ensuring that the total number of segments in the system is equal to the sum of the segment density distribution.

Solving the partial differential equation (eq 3), with the total potential defined through the segment volume distribution, produces the self-consistent solution. We use a numerical procedure similar to that of Dolan and Edwards,[12] where space is discretized into steps of length a, the segment size. An initial guess is taken for the distribution function (in our case, the ideal random walk distribution function[1,12]). Using this function we calculated the local segment density and insert it into the partial differential equation, leading to calculation of a new distribution function. Iterations were stopped when the relative difference between new and previous iteration segment distribution was less than 10^{-5}.

Once $Q(z,z';s)$ and the local segment density are obtained, system properties can be evaluated. The brush thickness is calculated from the second moment of the segment density distribution:

$$\langle L \rangle = \left\{ \frac{\int_0^{\infty} \phi_{tot}(z') z^2\, dz'}{\int_0^{\infty} \phi_{tot}(z')\, dz'} \right\}^{1/2} \quad (5)$$

Replacing ϕ_{tot} by ϕ_1 in this equation, we can calculate the average thickness of the inner brush, z_1.

The extent of the brush "foot" can be defined by the fraction of chain segments extending beyond L, as defined by eq 1:[15]

$$S_c(2) = \frac{\int_L^{\infty} \phi_{tot}(z)\, dz}{\int_0^{\infty} \phi_{tot}(z)\, dz} \quad (6)$$

To evaluate the extent of the inner brush "foot", $S_c(1)$, we replace L by the thickness of the inner brush, z_1 (eq 2), and ϕ_{tot} by ϕ_1.

The distribution of any segment, s, can be calculated as the normalized probability that a section, s segments long, starting at $z = 0$ and ending at z, will be followed by a section of $(N_i - s)$ segments, starting at z and ending anywhere in the brush:

$$\epsilon_i(s,z) = \frac{Q(0,z;s) \int_0^{\infty} Q(z,z';n_i-s)\, dz'}{\int_0^{\infty} Q(0,z;s)\, dz'} \quad (7)$$

where $i = 1$ or 2. Note that, although the distribution function $Q(z,z';s)$ is the same for both chains, $\epsilon_1(s,z)$ will not be equal to $\epsilon_2(s,z)$, because the summation over the "end" section depends on the value of N_i. The normalized distribution of chain ends can be obtained by substituting $s = N_i$ in eq 7. The average location of any segment s can be calculated from the distribution:

$$\langle \epsilon_i(s) \rangle = \left\{ \frac{\int_0^{\infty} \epsilon_i(s,z) z^2\, dz'}{\int_0^{\infty} \epsilon_i(s,z)\, dz'} \right\}^{1/2} \quad (8)$$

The segment distribution of two compressed brushes (see Figure 1), A and B, brought together within a distance d (in a units) is easily calculated by changing the integration limits in eq 1 to $0 \le z \le d$. The total segment density $\phi_{tot}(z)$ is, however, composed of $\phi_{tot}^{A}(z) + \phi_{tot}^{B}(d-z)$. The degree of interpenetration between two brushes can be defined[14] as the fraction of segments extending beyond the half-point:

$$I^{j}(d) = \frac{\int_{d/2}^{d} \phi_{tot}^{j}(z)\, dz}{\int_0^{d} \phi_{tot}^{j}(z)\, dz} \quad (9)$$

where j = A,B. For a symmetrical system, where brush A is identical to brush B, $I^{A}(d) = I^{B}(d)$. At surface separations that are much larger than $2L$, $I^{j}(d)$ is necessarily zero. However, as the brushes are brought closer together, the "feet" of the two brushes overlap and some interpenetration ensues, even though the overall segment density profile of the brush may be hardly perturbed.[14] Further compression can result either in stronger overlap or in compression and distortion of the segment density distributions. In the limit of infinite molecular weight, it is assumed that no interpenetration occurs,[8,9] so that I is equal to 0 for all d.

Because of the large number of variables in the system, we examined only systems where the overall surface density $\sigma = 0.1$. Numerical SCF calculations of monodisperse systems[14] have shown that the strong stretching assumption, inherent in these calculations, holds for σ values as low as 0.001 in chains of $N = 50$. We can therefore expect that if the surface density in the outer brush, $\sigma(1-f)$, and the molecular weight difference between the short and long chains $(N_2 - N_1)$ exceed these values, the outer brush would be stretched and our model would be valid. We did not consider the properties of the outer brush in systems where one of these conditions does not hold, i.e., when f is large or α is very small. However, the inner brush in such systems should not be greatly affected by the diluteness of the outer brush and can therefore be analyzed and compared to the analytical model predictions.

Results and Discussion

The normalized brush thickness, $\langle L \rangle / N_1$, is found to scale linearly with $\alpha(1-f)^{1/3}$, in agreement with eq 1[8,9,11] and the results of Monte Carlo simulations.[11] The normalized thickness of the inner brush, plotted in Figure 2 as a function of $(1 - (1-f)^{2/3})^{1/2}$, shows the predicted linear relationship (eq 2) only at intermediate f values; small deviations develop in the limit of $f \to 1$, and significant ones in the limit of $f \to 0$. The point of departure from the scaling of eq 2 in the latter case varies with the molecular weight ratio.

In the limit of high f, z_1 scales linearly with the short-chain molecular weight, in agreement with the analytical SCF model (Figure 3). The deviations observed in Figure 2 in this limit are due to an unpredicted dependence of z_1 on α. In the opposite limit of $f = 0$ (taken as 10^{-10} in our calculations) we find that the inner brush thickness scales not linearly with N_1, but with the free chain[1,2] radius of gyration, $N_1^{1/2}$. As in the high-f limit, z_1 varies significantly with α. Such deviations, in either limit, were not observed in the MC simulations of the bimodal brush,[11] since those were limited to moderate f values between 0.25 and 0.75.

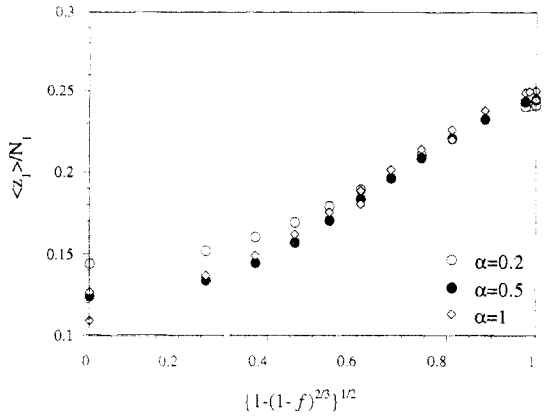

Figure 2. Normalized thickness of the inner brush, $\langle z_1 \rangle / N_1$, in units of a, as a function of $(1 - (1 - f)^{2/3})^{1/2}$ (eq 2).

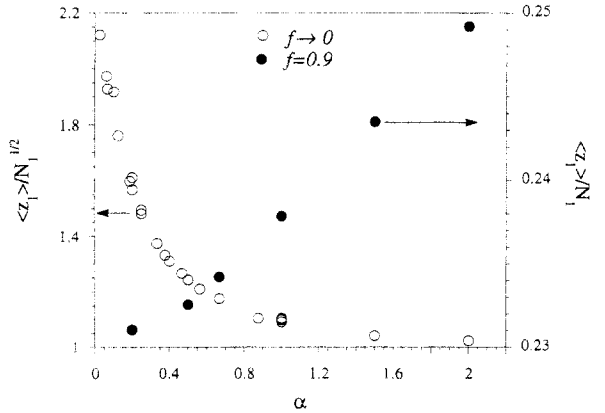

Figure 3. Thickness of the inner layer as a function of α: $\langle z_1 \rangle / N_1^{1/2}$ in the limit of low ($f = 10^{-10}$) fraction of short chains; $\langle z_1 \rangle / N_1$ in the limit of high ($f = 0.9$) fraction of short chains.

Figure 4 shows the segment density distribution and the chain end distribution as a function of distance from the surface. We see that the density profile of the shorter chains resembles a parabolic distribution, similar to profiles calculated for monodisperse, finite molecular weight brushes.[14,15] However, the density distribution of the longer chains is characterized by a "plateau" extending throughout the inner layer, which has been observed to some extent in the MC simulations as well.[11] This profile indicates that the longer chains are more stretched in the inner layer than the shorter chains. Vertical segregation can be seen even more clearly in the distribution of chain ends: The longer chain ends are localized at the outer edge of the brush, while the shorter chain ends concentrate in the inner layer. There is a crossover region, corresponding to the inner layer foot, where ends of both short and long chains coreside. In the limit of high f, when most of the chains are short and $\langle L \rangle \approx z_1$, we see that the longer chain ends are localized in a relatively narrow region in the outer brush edge. The width of the distribution of longer chain ends decreases, in general, with increasing molecular weight of both chains and with decreasing α.

Comparing the average location of the N_1 segment of both long and short chains verifies the difference in degrees of stretching (Figure 5a): The average location of the N_1 segment of the longer chains is higher than that of the same segment in the shorter chains for all values of f. In the limit of $f \rightarrow 1$ the small fraction of longer chains stretch through the inner layer, thereby decreasing the interaction energy. The degree of stretching and, hence, the ratio between the height of the N_1th segment of the short and long chains are limited by the significant entropy loss associated with stretching the longer chains. In the opposite limit, where $f \rightarrow 0$, the shorter chains adopt the smaller $N_1^{1/2}$ dimensions, and the ratio between the two degrees of stretching can become much higher. Figure 5b shows the average height of the chain ends as a function of brush composition. We see that the longer chain ends are distributed at the outer edge of the brush, while the shorter chain ends are located in the interior. The average height of both the long- and the short-chain ends increases with f. It should be noted that, contrary to predictions, the distribution of short-chain ends does seem to depend on α.

The extent of the brush foot is a measure of deviations from the analytical, infinite molecular weight limit[5,14,15] and is predicted to scale[5] in monodisperse brushes as $(\sigma^{1/3}N)^{-1/3}$. In Figure 6a we see that the overall bimodal brush foot (eq 6) does decrease with $N_2^{1/3}$ However, the expected $(1 - f)^{-1/9}$ variation is not observed; $S_c(2)$ seems to be independent of either f or α. Although the inner brush foot scales, as expected, with $N_1^{-1/3}$, a significant and nonlinear dependence on both α and f is observed (Figure 6b). Such a dependence was not seen in the MC simulations,[11] which concentrated on systems with a large molecular weight difference ($\alpha \geq 0.5$), where the variation of $S_c(1)$ with α is no longer strong.

The segment density profile of two compressed brushes is shown in Figure 7, as a function of distance between surfaces (d). The brushes are symmetrical, namely, σ, f, N_1, and N_2 are identical. The longer chains readily interpenetrate, even at relatively large distances between surfaces. At high compression ($d = 70$), when $d \ll 2L$, the longer chains are still stretched through the inner brush, as indicated by the "plateau" region. The persistence of vertical segregation under compression is seen, even more clearly, when examining the distribution of chain ends (Figure 8). At large separations there is some overlap between the long chain ends distribution, but none between the short chains. As d decreases, the longer chain ends of the two brushes overlap rather than retreat into the inner brush. The short chains, though, hardly interpenetrate, and there is very little overlap in the distribution of short-chain ends.

In Figure 9 the degree of interpenetration between two symmetric brushes is shown as a function of surface separation. There seems to be no significant difference in the degree of interpenetration between bimodal brushes of various composition and molecular weight and the interpenetration between two monodisperse brushes of equivalent length, N_e, where $N_e = fN_1 + (1 - f)N_2$. This, however, is somewhat curious since the uncompressed brush foot does not depend on either f for α (Figure 6A).

Conclusions

We have investigated the properties of a bimodal brush, using a numerical solution to the SCF model. This procedure allows us to examine the properties of high, but finite, molecular weight systems, which can be easily examined neither by simulations[10,11] nor by analytical theory.[8,9] We can thereby investigate the effect of finite chain molecular weight on system properties and estimate the importance of these deviations.

Vertical segregation between segments of the longer and shorter chains is clearly seen, irrespective of brush composition or molecular weight ratio. The stratification of long- and short-chain segments, even in the limit of low α, indicates that a small degree of polydispersity can significantly alter the inner structure of the brush. The longer chain ends are, to a large extent, confined to the region outside the inner brush, so that in systems of low α or high f where z_1 approaches the overall thickness L,

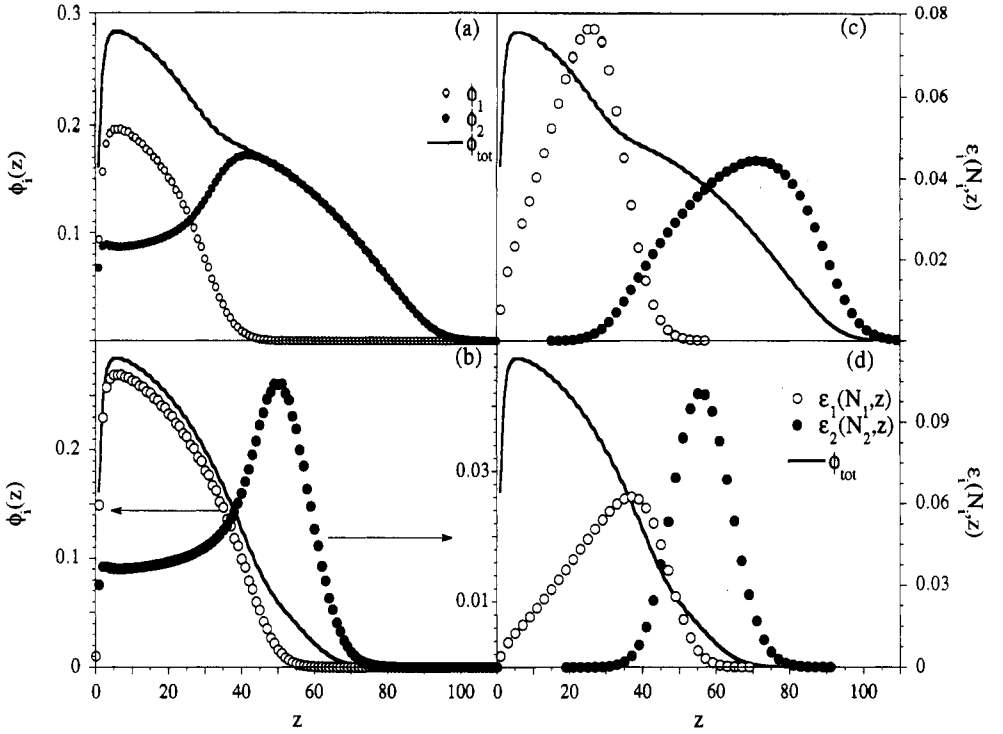

Figure 4. Volume and chain end distrubutions as a function of distance from the grafting surface, z. (a) Volume fraction distribution of the short, long, and overall segments (eq 4) as a function of z. $N_1 = 100$, $\alpha = 1$, and $f = 0.5$. (b) Volume fraction distribution of short, long, and overall segments (eq 4) as a function of z. The symbols are as set in (a). $N_1 = 100$, $\alpha = 0.5$, and $f = 0.9$. (c) Short and long chain end distribution of the brush described in (a) as a function of z (eq 7). The overall segment distribution, $\phi_{tot}(z)$, is not drawn to scale. (d) Chain end distribution of short and long chains of the brush described in (b) as a function of z. The overall segment distribution, $\phi_{tot}(z)$, is not drawn to scale.

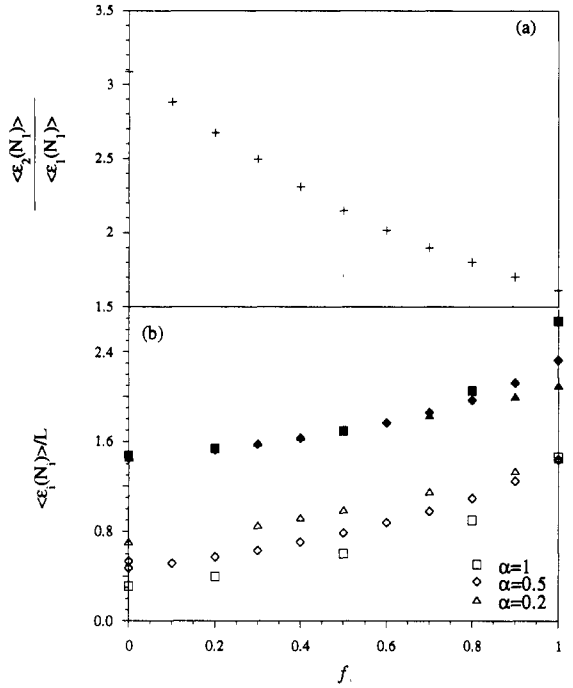

Figure 5. Differences in short- and long-chain stretching in the bimodal brush. $\langle \epsilon_i(s) \rangle$ is calculated from eq 7. (a) Ratio of the average location of the N_1 segment of the long and short chains as a function of f. $N_1 = 100$ and $\alpha = 0.5$. (b) Average location of short- and long-chain ends in the brush. Open symbols denote the short-chain ends, and full symbols the long-chain ends. $\langle L \rangle$ is calculated from eq 5.

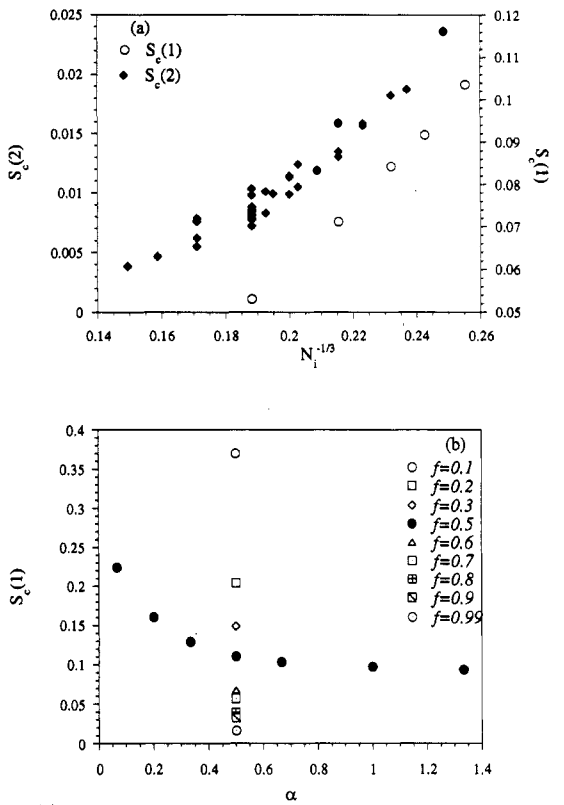

Figure 6. Overall and inner brush foot as calculated by eq 6: (a) Overall brush foot, $S_c(2)$, as a function of $N_2^{-1/3}$, for various values of α and f, and the inner brush foot $S_c(1)$ as a function of $N_1^{-1/3}$, for $\alpha = 1$ and $f = 0.5$. (b) $S_c(1)$ as a function of f and α. $N_2 = 150$.

the longer chain ends are confined to a relatively narrow strip at the outer edge of the brush. Functionalization of the longer chain ends in such systems will allow modification of the outer brush edge without affecting the internal brush structure.

The overall brush thickness is found to scale as $N_1(1 + \alpha(1 - f)^{1/3})$, in agreement with the analytical SCF model (eq 1).[8,9] This scaling is also in good agreement with recent experiments[16] where the range of surface forces generated

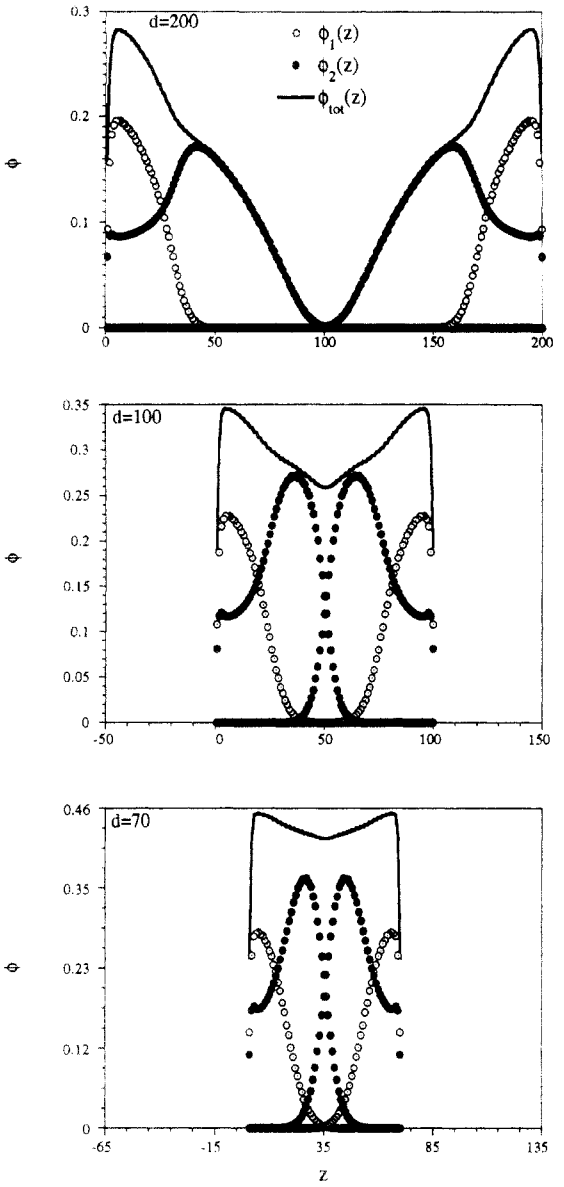

Figure 7. Effect of compression on brush segment density distribution. The brushes are symmetrical. $N_1 = 100$, $\alpha = 1$, and $f = 0.5$. L (as calculated by eq 1) is equal to 88.9.

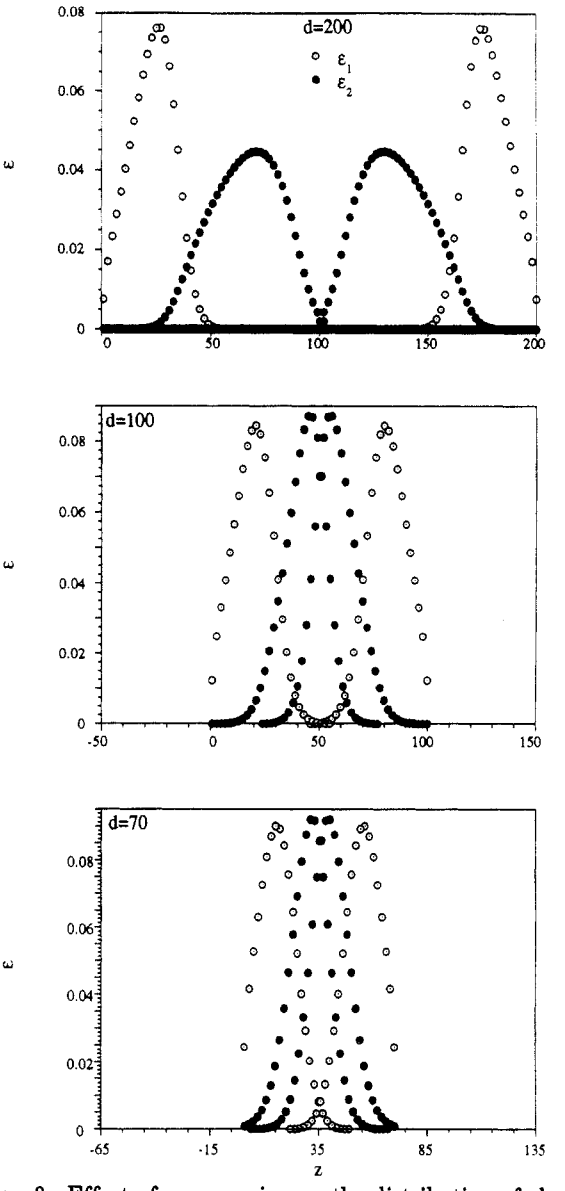

Figure 8. Effect of compression on the distribution of chain ends for the brush described in Figure 7.

by bimodal brushes were measured. The outer brush foot was found to decrease linearly with $N_2^{-1/3}$ and to be independent of both α and f. This is rather surprising, since the bimodal brush foot should have decreased[5] with the surface density of the longer chains, i.e., $(1 - f)$, to the power of 1/9. The outer bimodal brush foot, which largely determines the response to flow,[6] is therefore independent of the shorter chain properties.

The inner brush thickness deviates from the predicted scaling of eq 2 in the limit of both low and high f values. Especially significant are the deviations when $f \to 0$, where the shorter chains adopt an unstretched configuration. The deviations from the asymptotic limit[8,9] due to finite molecular weight effects, as exhibited by the inner layer foot, decrease with $N_1^{-1/3}$. This is as expected from comparison to monodisperse systems.[5,14,15] There is, however, a strong and unpredicted dependence of the inner brush foot on composition and molecular weight ratio, which has not been observed in the MC simulations.[11] These deviations may be explained by the presence of longer chain segments at the outer edge of the inner brush: A chain segment venturing away from a monodisperse brush (or the outer brush edge in the bimodal brush) encounters nearly pure solvent and is therefore

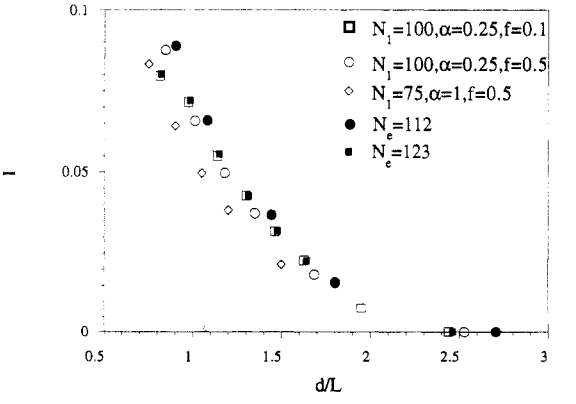

Figure 9. Interpenetration between brushes, defined in eq 9, as a function of distance between surfaces, compared to the interpenetration between monodisperse brushes of $N_e = fN_1 + (1 - f)N_2$. For $N_1 = 75$, $\alpha = 1.0$, and $f = 0.5$, $N_e = 112$. For $N_1 = 100$, $\alpha = 0.25$, and $f = 0.5$, $N_e = 112$. For $N_1 = 100$, $\alpha = 0.25$, and $f = 0.1$, $N_e = 123$.

driven out by the potential gradient between the brush edge and the solvent. However, a short-chain segment extending beyond the inner brush encounters segments from the longer chains, and the potential gradient is therefore much smaller. As the molecular weight ratio

decreases, or f increases, the outer brush becomes smaller and more dilute, enabling easier interpenetration from the inner brush.

The vertical segregation between the molecular weights is extremely stable: under compression, stratification persists. The degree of interpenetration between two bimodal brushes is similar to the interpenetration between two brushes of equivalent molecular weight. The ratio of bimodal brush thickness (L) to the equivalent, monodisperse brush thickness is $\{1 + \alpha(1 - f)^{1/3}\}/\{f + \alpha(1 - f)\}$ and for moderate α values is quite close to 1 for all f. This leads us to an interesting conclusion: The interactions between bimodal brushes, and their layer thickness, will be the same as those of an equivalent monodisperse brush, but their inner structure will differ significantly. The outer surface would remain, throughout compressions and expansions, dominated by the longer chain ends.

Acknowledgment is made to the donors of the Petroleum Research Fund, administered by the American Chemical Society, for the partial support of this research. Partial support was also received, with appreciation, from the National Science Foundation (Grant NSF/CTS-9107025, Interfacial Transport and Separations Program (CTS) and Polymers Program (DMR)). This research was partiallysupported by a grant of computer time from the Minnesota Supercomputer Institute. We would like to thank S. Prager, S. T. Milner, J. F. Argillier, E. E. Parsonage, and S. Dhoot for helpful discussions.

References and Notes

(1) Halperin, A.; Tirrell, M.; Lodge, T. P. *Adv. Polym. Sci.* **1992**, *100*, 31.
(2) Milner, S. T. *Science* **1991**, *252*, 905.
(3) Alexander, S. *J. Phys. (Paris)* **1976**, *38*, 977.
(4) De Gennes, P.-G. *Macromolecules* **1980**, *13*, 1069.
(5) Witten, T. A.; Leibler, L.; Pincus, P. A. *Macromolecules* **1990**, *23*, 824.
(6) Fredrickson, G. H.; Pincus, P. A. *Langmuir* **1991**, *7*, 786.
(7) Tirrell, M.; Parsonage, E.; Watanabe, H.; Dhoot, S. *Polym. J.* **1991**, *23*, 641.
(8) Milner, S. T.; Witten, T. A.; Cates, M. *Macromolecules* **1989**, *22*, 853.
(9) Birshtein, T. M.; Liatskaya, Y. V; Zhulina, E. B. *Polymer* **1990**, *31*, 2185.
(10) Chakrabarti, A.; Toral, R. *Macromolecules* **1990**, *23*, 2016.
(11) Lai, P. Y.; Zhulina, E. B. *Macromolecules* **1992**, *25*, 5201.
(12) Dolan, A. K.; Edwards, S. F. *Proc. R. Soc.* **1975**, *A343*, 427.
(13) Milner, S. T.; Witten, T. A.; Cates, M. *Macromolecules* **1988**, *21*, 2610.
(14) Patel, S. S. Talk presented at "Tethered Chains I: A Symposium on the Science of Polymeric Surfactants", Minneapolis, May 1991.
(15) Milner, S. T. *J. Chem. Soc., Faraday Trans.* **1990**, *86*, 1349.
(16) Dhoot, S.; Watanabe, H.; Tirrell, M. *Polym. Prepr. (Am. Chem. Soc., Div. Polym. Chem.)* **1993**, *34* (2), 290.